J. Phys.: Condens. Matter **8** (1996) L215–L221. Printed in the UK

LETTER TO THE EDITOR

Internal forces and the magnetoconductivity of a nondegenerate 2D electron fluid

P Fozooni†, P J Richardson†, M J Lea†, M I Dykman‡, C Fang-Yen§¶ and A Blackburn‖

† Department of Physics, Royal Holloway, University of London, Egham, Surrey TW20 0EX, UK

‡ Department of Physics and Astronomy, Michigan State University, MI 48824, USA

§Department of Physics, Stanford University, Stanford, CA 94305, USA

‖ Department of Electronics and Computer Science, University of Southampton, Southampton SO17 1BJ, UK

Received 19 February 1996

Abstract. The forces on individual electrons in an unscreened nondegenerate electron fluid, due to electron density fluctuations, have been calculated using Monte Carlo simulations and determined experimentally over a broad range of the plasma parameter Γ. The experimental results are obtained from the magnetoconductivity $\sigma(B)$ measured for electrons on liquid helium below 1 K for $B \leqslant 8$ T. The magnitude and density dependence of $\sigma(B)$ are explained by the many-electron theory of magnetotransport. The internal electric fields found from the experiments are in excellent agreement with the simulations.

Electrons above the surface of superfluid helium often form a two-dimensional (2D) *normal fluid* [1]: for characteristic electron densities $n \sim 10^{12}$ m^{-2} the interelectron distance $\sim n^{-1/2}$ exceeds the de Broglie wavelength, and the system is nondegenerate; at the same time, the ratio of the characteristic Coulomb energy of electron–electron interaction to the kinetic energy, the plasma parameter $\Gamma = e^2(\pi n)^{1/2}/4\pi\epsilon_0 kT$ is large, and therefore there is short-range order in the electron system [2]. For $\Gamma > 127$ (low T) electrons form a 2D crystal [3]. Mean-field effects such as long-wavelength plasma oscillations are well understood for a normal 2D electron liquid [4] but much less is known about the detailed behaviour of individual electrons. An experimental probe is required while, on the theoretical side, the problem is complicated by the absence of 'good' quasiparticles.

In this letter, we present data from Monte Carlo simulations and experimental measurements of an important but unexplored characteristic of a 2D electron fluid, the internal electric field $\boldsymbol{E}_f$ that drives an electron as a result of its interaction with other electrons. Unlike the long-wavelength fluctuational fields known in plasma physics [5], the field $\boldsymbol{E}_f$, although also of fluctuational origin, determines the force driving an *individual particle*, and is not described by the theory [5]. The force on a particle is an important dynamical characteristic of a system. In 'conventional' fluids with short-range interatomic interaction, the forces have been a subject of extensive research [6]. The mean square force remains finite in a fluid (though the mean square displacement diverges), but it would be expected to display singular behaviour at the liquid–crystal transition.

¶ Now at Department of Physics, MIT, Cambridge, MA 02139, USA.

0953-8984/96/130215+07$19.50

A special significance of the field $\boldsymbol{E}_f$ for a nondegenerate 2D electron system stems from the fact that, over a broad range of parameters, it strongly affects magnetotransport. In the single-particle approximation the electron energy spectrum in a magnetic field B perpendicular to the electron layer consists of discrete Landau levels, separation $\hbar\omega_c$ ($\omega_c = eB/m$ is the cyclotron frequency). The centres of the cyclotron orbits move only because of the random potential of the scatterers. Therefore scattering is always strong, and the pattern of transport is very different from the standard Drude picture which applies for weak coupling at $B = 0$ and in which scattering events are short and well separated in time.

The field $\boldsymbol{E}_f$ causes the centres of the cyclotron orbits to drift at a velocity E_f/B, and may 'restore' the weak-coupling picture. This effect was first discussed and investigated [7] for transport in the quantum limit $\hbar\omega_c/kT \gg 1$. It was shown later [8, 9] that the field $\boldsymbol{E}_f$ also dramatically affects the magnetoconductivity $\sigma(B)$ in classically strong magnetic fields, $\mu B \gg 1, \hbar\omega_c/kT < 1$ (μ is the zero-field electron mobility), for vapour-atom scattering above 1 K. In particular, it restores the Drude-type behaviour of $\sigma(B)$ for comparatively small B which has been known experimentally since [10]. Cyclotron resonance measurements [11] have also demonstrated the importance of Coulomb interactions in this system. Several other mechanisms have been proposed to explain previous measurements of $\sigma(B)$ at higher B [12].

Our new measurements of $\sigma(B)$ have been done below 1 K, in the ripplon scattering regime. In this range the mobility μ is extremely high ($\lesssim 2000$ m^2 V^{-1} s^{-1}), enabling *quantitative* characterization of $\boldsymbol{E}_f$ as a function of density and temperature.

We consider the distribution of $\boldsymbol{E}_f$ for a classical normal liquid; the results also apply for quantizing magnetic fields provided the motion of the centres of the cyclotron orbits is semiclassical. Since fluctuations in the system are thermal, and the field is due to electron–electron interaction, the scale for $\boldsymbol{E}_f$ is given by the characteristic field E_0:

$$\langle \boldsymbol{E}_f^2 \rangle = F(\Gamma) E_0^2 \qquad E_0 = \left(kTn^{3/2}/4\pi\epsilon_0\right)^{1/2}. \tag{1}$$

The scaled dimensionless mean square field $F(\Gamma)$ can be easily found for large Γ (low T) in the 2D crystal phase [13]. Here, the force on an electron $e\boldsymbol{E}_f$ arises because of the displacement of electrons from their lattice sites $\boldsymbol{R}_n$. In the harmonic approximation the force is linear in the displacements and has a Gaussian distribution. The function F incorporates contributions from both transverse and longitudinal modes of the crystal, and $F(\Gamma) \approx 8.91$, independent of Γ.

In the opposite limit of a nearly ideal plasma, $\Gamma \ll 1$, the major contribution to the force on an electron originates from pair collisions, which gives $F(\Gamma) \approx 2\pi^{3/2}/\Gamma$.

In the most interesting range of the electron liquid and the melting transition, the function $F(\Gamma)$ was obtained from Monte Carlo simulations. We used the Metropolis algorithm and the Ewald summation technique following Gann *et al* [2], with periodic boundary conditions. The field on an electron was evaluated as the gradient of the potential in which the electron was moving.

The results for $\boldsymbol{E}_f$ for the number of particles $N = 196,\ 324$ are very close to each other. In the range $\Gamma > 30$ the probability density distribution ρ of the field components E_x and E_y is close to Gaussian. The functions $F(\Gamma)$ and ρ are plotted in figure 1. The scaling function $F(\Gamma)$ decreases nearly monotonically with increasing Γ. However, remarkably, its variation is *very small* in the range $\Gamma \gtrsim 10$, although the structure of the system changes dramatically, from a crystal to a liquid with a correlation length of twice the mean electronic separation. The function $F(\Gamma)$ has a smeared singularity at the melting point. Detailed discussion will be given elsewhere [14].

The magnetoconductivity of 2D electrons above superfluid helium was measured using

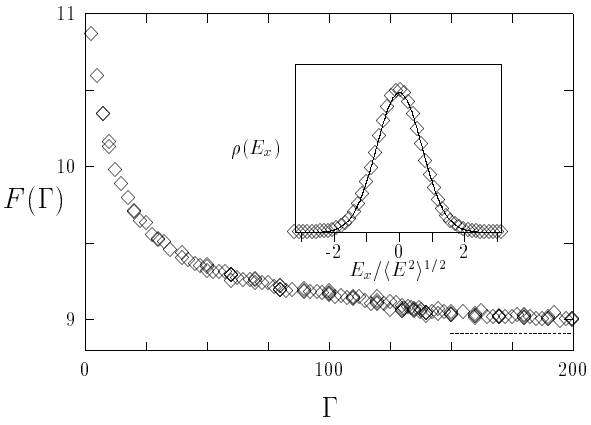

Figure 1. The scaled mean square field $F(\Gamma)$ from Monte Carlo calculations. The asymptotic value of F for a harmonic Wigner crystal is shown dashed. Inset, the field component distribution.

4 mm diameter Corbino disc electrodes (see figure 2) 100 μm beneath the electrons [9]. Free electrons were held over the central drive electrode **A**, a ring electrode **E**, and receiving electrodes **B1**, **B2** and **B3** surrounded by a planar guard **G**. An ac voltage V_0 (typically 10 mV) at a frequency up to 10 kHz was applied to electrode **A** and the ac currents I to the electrodes **B** measured. For a perfect conductor the phase of the capacitively coupled current I is $\pi/2$ with respect to V_0. The phase shift $\phi(B)$ away from $\pi/2$ was measured for perpendicular magnetic fields $B \leqslant 8$ T for electron densities $0.5 \times 10^{12} \lesssim n \lesssim 2 \times 10^{12}$ m^{-2} at temperatures $0.6 \lesssim T \lesssim 0.9$ K in the fluid phase. The phase shift $\phi(B)$ is proportional to $\sigma^{-1}(B)$ for $\phi \lesssim 0.3$ rad, while for larger phase shifts the theoretical response function was used. The density n was determined from the negative dc bias voltage on electrode **E** required to cut off the current between electrodes **A** and **B**.

Figures 2 and 3 show the measured magnetoconductivity for several densities and temperatures. In low fields, $B < 0.5$ T, the data accurately follow the simple Drude-like result, even for values of μB as large as 500:

$$\sigma(B) = \frac{\sigma(0)}{1 + (\mu B)^2} \qquad \frac{ne}{\mu\sigma(B)} \approx B^2 \qquad \text{for } \mu B \gg 1. \tag{2}$$

The electron mobility was determined from the B^2 dependence of $\sigma^{-1}(B)$, as a function of density and temperature, and is in excellent agreement with previous $B = 0$ measurements by Mehrotra *et al* [15]. The measured mobilities from 0.6 to 0.9 K are close to the theoretical values for a classical strongly correlated electron liquid [14], with scattering by both ripplons and ^{4}He vapour atoms taken into account [16]. The mobility is slightly density dependent, primarily because the electric field that presses electrons against the helium surface increases with n, and therefore so does the electron–ripplon coupling. The data are plotted as $ne/\mu\sigma(B)$ against B (figure 2) or B^2 (figure 3) using the experimental values of μ for each n and T. For $B < 0.5$ T the data lie on the *universal* line, $ne/\mu\sigma(B) = B^2$ (line **a** in figures 2 and 3).

At this point we should stress that the simple-minded Drude model (2) effectively applies *because of the internal electric fields* [8, 14]. To understand the effect qualitatively, we notice that the many-electron system transfers its momentum to short-range scatterers

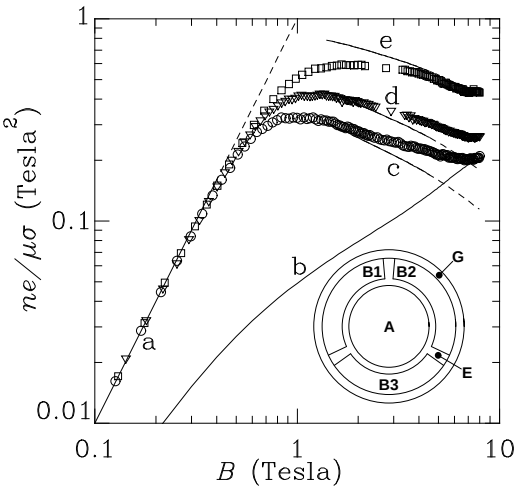

Figure 2. $ne/\mu\sigma(B)$ versus B for $n = 0.55$ (○), 0.88 (▽) and 1.89 (□) $\times 10^{12}$ m^{-2} at 0.7 K. The mobility $\mu = 985$, 830 and 520 ± 20 m^2 V^{-1} s^{-1}, respectively. Solid lines **a** (low B) and **c**–**e** (high B) show many-electron calculations. Inset, the Corbino electrode geometry.

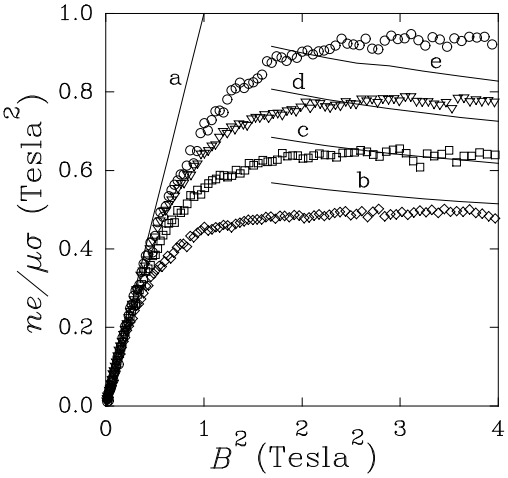

Figure 3. $ne/\mu\sigma(B)$ versus B^2 for $T = 0.6$ (◇), 0.7 (□), 0.8 (▽) and 0.9 K (○). The mobility $\mu = 755$, 620, 430 and 250 ± 15 m^2 V^{-1} s^{-1}, respectively. Lines **a** (low B) and **b**–**e** (high B) show many-electron calculations.

via individual electron–scatterer collisions. In a certain range of the parameters, all that an electron 'knows' about other electrons during a collision is the field $\boldsymbol{E}_f$, and this field is time independent if the collision is short enough. Then the Einstein relation for the conductivity applies:

$$\sigma(B) = ne^2L^2\tau^{-1}(B)/kT \tag{3}$$

where $L \equiv L(B)$ is the diffusion length and $\tau^{-1}(B)$ is the relaxation rate. For $\mu B \gg 1$ the diffusion length is given by the mean radius $\bar{R}$ of the cyclotron orbit, $L^2 = \bar{R}^2/2 = (\bar{h}/2eB)(2\bar{n} + 1)$, with $\bar{n} = 1/[\exp(\bar{h}\omega_c/kT) - 1]$.

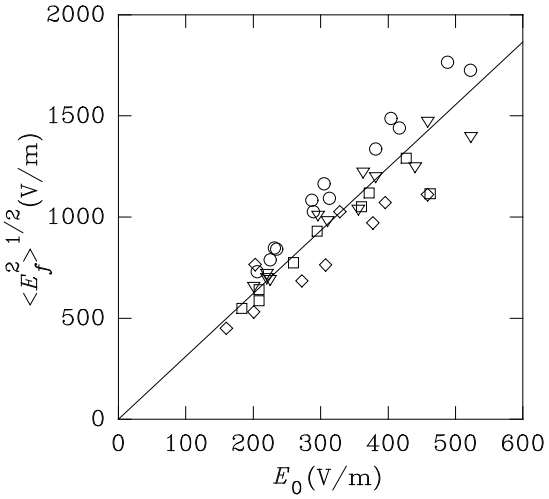

Figure 4. Values of the internal field $\langle \boldsymbol{E}_f^2 \rangle^{1/2}$ versus E_0 at 0.6 (◇), 0.7 (□), 0.8 (▽) and 0.9 K (○). The solid line shows the best linear fit with $\langle \boldsymbol{E}_f^2 \rangle^{1/2} = 3.11 E_0$.

It is the relaxation rate in (3) that is primarily affected by internal electric fields. For $kT \gg eE_f \bar{\lambda}_T > \hbar\omega_c$ ($\bar{\lambda}_T = \hbar/(2mkT)^{1/2}$) the field $\boldsymbol{E}_f$ smears out the Landau levels and thus *eliminates* the effects of their discreteness. Therefore $\tau^{-1}(B) = \tau^{-1}(0)$, and the B dependence of σ is given by that of $L^2 = mkT/e^2B^2 \propto B^{-2}$, i.e. the many-electron theory gives $en/\mu\sigma$ independent of n as observed (cf the solid line **a** in figures 2 and 3). In contrast, in the single-electron picture the relaxation rate is increased by the density of states enhancement factor $\omega_c\tau(B)$, since the states in the energy strip $\hbar\omega_c$ are 'compressed' down to the Landau level collision width $\hbar\tau^{-1}(B)$. The total magnetoconductivity from the self-consistent Born approximation (SCBA) for ripplon [16] and gas-atom scattering [17] and their self-consistent combination $\sigma_s = (\sigma_{rs}^2 + \sigma_{gs}^2)^{1/2}$ is plotted (line **b**) in figure 2 for $n = 0.55 \times 10^{12}\text{m}^{-2}$ and $T = 0.7$ K. At 2 T, the SCBA overestimates $\sigma(B)$ by an order of magnitude.

A distinctive feature of the classical $\sigma(B)$ is *saturation* with increasing B. This arises because an electron in crossed $\boldsymbol{E}_f$ and $\boldsymbol{B}$ fields moves along a spiral with a step $\sim 2\pi E_f/B\omega_c$. The number of times it encounters a short-range scatterer in the classically strong field B is then $N_{enc} \sim \bar{\lambda}_T B\omega_c/2\pi E_f$ ($\bar{\lambda}_T$ is the uncertainty in the position of an electron). For $N_{enc} > 1$ one would expect the scattering rate, and thus $\sigma(B)$, to increase by a factor $\sim N_{enc} \propto B^2$, and we find (cf equation (2))

$$\frac{ne}{\mu\sigma(B)} \approx \pi B_0^2 \qquad B_0^2 = \left(\frac{2m^3kT}{e^2\hbar^2}\right)^{1/2} \langle \boldsymbol{E}_f^2 \rangle^{1/2}. \tag{4}$$

The saturation of $ne/\mu\sigma(B)$ is clearly seen in figures 2 and 3 for $B > 1.0$ T. The limiting value of $ne/\mu\sigma(B)$ increases with density (figure 2) and temperature (figure 3) and is directly proportional to the rms internal electric field, from (4). It is this which enables the internal field to be determined experimentally.

For $B \gtrsim 1$ T quantum effects become substantial. For $\hbar\omega_c \gg kT$ the diffusion length $L \approx (\hbar/2eB)^{1/2}$, and also $N_{enc} \sim (\hbar/eB)^{1/2} B\omega_c/2\pi E_f$, so that $ne/\mu\sigma(B) \propto B^{-1/2}$ decreases with increasing B. For higher $B \gtrsim 5$ T (depending on n and T) the duration of a collision $\tau_{col} \gtrsim \tau(B)$ and this theory no longer applies.

Equation (4) is written [8] for short-range scatterers (such as helium vapour atoms). In the case of scattering by ripplons, an extra factor arises which is numerically close to unity for the experimental conditions here. Calculations of the magnetoconductivity for gas-atom and ripplon scattering were made using the full semiclassical many-electron theory in the range $\hbar\omega_c \gtrsim kT$ [14], with values of $\langle \boldsymbol{E}_f^2 \rangle$ taken from figure 1. The results for the total many-electron magnetoconductivity $\sigma_m = \sigma_{rm} + \sigma_{gm}$ are shown in figure 2 (lines **c**–**e**, increasing n) and figure 3 (lines **b**–**e**, increasing T), and show satisfactory agreement with the experiments for $\tau_{col} \ll \tau(B)$ (the extrapolation of the theoretical curves to the range $\tau_{col} \sim \tau(B)$ is shown dashed).

Conversely, the measured $\sigma^{-1}(B)$ at $B = 2$ T was used to obtain experimental values of the internal electric fields. This value of B is within the range of the applicability of the theory ($kT > eE_f(\hbar/eB)^{1/2}$; $\hbar\omega_c > kT$) and is also far from the Drude region and the region where collisional level broadening affects the scattering. The experimental values of $\langle \boldsymbol{E}_f^2 \rangle^{1/2}$ against E_0 are shown in figure 4 (we renormalized E_0 in (1) to allow for the dielectric constant of liquid helium). The points are from over 40 combinations of density and temperature between 0.6 and 0.9 K where the conductivity varies by more than an order of magnitude; no adjustable parameters have been used, and so the spread of the points may be considered to be within reasonable limits. Within the errors the measured field is proportional to E_0, with a constant of proportionality $\nu = 3.11 \pm 0.10$. This can be compared with $F^{1/2} = 3.07 \pm 0.03$ from the Monte Carlo simulations for the range $20 < \Gamma < 70$ covered by the experiments. A slight decrease of ν with decreasing T seen in figure 4 lies within the errors.

In conclusion, we have both computed and measured the internal electric fields in a nondegenerate 2D electron fluid, and the results are in excellent agreement. We show that, over a broad range of parameters, the magnitude and density dependence of the magnetoconductivity $\sigma(B)$ of electrons on helium are determined by many-electron effects and can be understood qualitatively in terms of electron diffusion controlled by a fluctuational internal electric field.

We thank R van der Heijden, P Sommerfeld and O Tress for useful discussions; the EPSRC (UK) for a research grant and for a studentship (for PJR); the EU for support under contract CHRXCT 930374; A K Betts, F Greenough and J Taylor for technical assistance; D Murphy, A Jury and the staff of the Southampton University Microelectronics Centre and the lithography unit of the Rutherford Appleton Laboratory.

References

[1] Wyatt A F G and Lauter H J (eds) 1991 *Excitations in Two-Dimensional and Three-Dimensional Quantum Fluids* (New York: Plenum)
Andrei E (ed) 1987 *2D Electron Systems on Helium and Other Substrates* (New York: Kluwer)
For an introductory review see Vinen W F and Dahm A J 1987 *Phys. Today* **40** 43

[2] Gann R C, Chakravarti S, and Chester G V 1979 *Phys. Rev.* B **20** 326
Hansen J P, Levesque D and Weiss J J 1979 *Phys. Rev. Lett.* **43** 979

[3] Grimes C C and Adams G 1979 *Phys. Rev. Lett.* **42** 795
Fisher D S, Halperin B I and Platzman P M 1979 *Phys. Rev. Lett.* **42** 798
Shirahana K and Kono K 1995 *Phys. Rev. Lett.* **74** 781

[4] Grimes C C and Adams G 1976 *Phys. Rev. Lett.* **36** 145
Mast D B, Dahm A J and Fetter A L 1985 *Phys. Rev. Lett.* **54** 1706
Glattli D C, Andrei E, Deville G, Pointrenaud G and Williams F I B 1985 *Phys. Rev. Lett.* **54** 1710
Peeters P J M, Lea M J, Janssen A M L, Stone A O, Jacobs W P N M, Fozooni P and van der Heijden R W 1991 *Phys. Rev. Lett.* **67** 2199

[5] Krall N A and Trivelpiece A W 1973 *Principles of Plasma Physics* (New York: McGraw-Hill)
[6] Croxton C A 1974 *Liquid State Physics—a Statistical Mechanical Introduction* (Cambridge: Cambridge University Press)
[7] Dykman M I and Khazan L S 1979 *Sov. Phys.–JETP* **50** 747
Dykman M I 1980 *Sov. J. Low Temp. Phys.* **6** 268
Frost J, Fozooni P, Lea M J and Dykman M I 1991 *Europhys. Lett.* **16** 575
[8] Dykman M I, Lea M J, Fozooni P and Frost J 1993 *Phys. Rev. Lett.* **70** 3975
Lea M J and Dykman M I 1994 *Phil. Mag.* B **69** 1059
[9] Lea M J, Fozooni P, Richardson P J and Blackburn A 1994 *Phys. Rev. Lett.* **73** 1142
[10] Iye Y 1980 *J. Low Temp. Phys.* **40** 441
[11] Edel'man S 1979 *Sov.Phys.–JETP* **50** 338
Wilen L and Giannetta R 1988 *Phys. Rev. Lett.* **60** 231
[12] Kovdrya Yu Z, Nikolayenko V A, Kirichek O I, Sokolov S S, and Grigor'ev V N 1993 *J. Low Temp. Phys.* **91** 371
Neuenschwander J, Joss W and Wyder P 1992 *Helv. Phys. Acta* **65** 325; 1994 *Physica* B **194-196** 1231
[13] Dykman M I 1982 *J. Phys. C: Solid State Phys.* **15** 7397
[14] Dykman M I, Fang-Yen C and Lea M J to be published
[15] Mehrotra R, Guo C J, Ruan Y Z, Mast D B and Dahm A J 1984 *Phys. Rev.* B **29** 5239
[16] Saitoh M 1977 *J. Phys. Soc. Japan* **42** 201; 1984 *Solid State Commun.* **52** 63
Buntar' V A, Kovdrya Yu Z, Grigoriev V N, Monarhka Yu P and Sokolov S S 1987 *Sov. J. Low Temp. Phys.* **13** 451
[17] Ando T, Fowler A B and Stern F 1982 *Rev. Mod. Phys.* **54** 437
van der Heijden R W, van de Sanden M C M, Surewaard J H G, de Waele A Th A M, Gijsman H M and Peeters F M 1988 *Europhys. Lett.* **6** 75
Peters P J M, Scheuzger P, Lea M J, Monarkha Yu P, Sommerfeld P K H and van der Heijden R W 1994 *Phys. Rev.* B **50** 11570